

PAPER • OPEN ACCESS

Effect of Texture Depth on the Hydrodynamic Performance of Lubricated Contact Considering Cavitation

To cite this article: Nazaruddin Sinaga *et al* 2019 *IOP Conf. Ser.: Mater. Sci. Eng.* **494** 012047

View the [article online](#) for updates and enhancements.



IOP | ebooksTM

Bringing you innovative digital publishing with leading voices to create your essential collection of books in STEM research.

Start exploring the collection - download the first chapter of every title for free.

Effect of Texture Depth on the Hydrodynamic Performance of Lubricated Contact Considering Cavitation

Nazaruddin Sinaga^{1*}, Mohammad Tauviqirrahman¹, Arif Rahman Hakim¹, Eflita Yohana¹

¹Department of Mechanical Engineering, Diponegoro University, Semarang, Indonesia

*Corresponding author: nazarsinaga@undip.ac.id

Abstract. Surface texturing on the lubricated bearing has proven to enhance the hydrodynamic performance. The present work explores the influence of texture parameter as well as the Reynolds number on the tribological performance using computational fluid dynamic (CFD) approach. The inclusion of cavitation model in the analysis of lubrication performance is of particular interest. It is shown that the cavitation has a significant effect on the hydrodynamic pressure, and thus the cavitation model should be considered in analysis. Moreover, in this study the optimal relative texture depth is discussed in more detail regarding with the cavitation effect.

Keywords: cavitation, computational fluid dynamic, CFD, lubrication, texturing

1. Introduction

Recently, the study of texturing of the lubricated contact has obtained an explosion interest by researchers around the world. It is known that by introducing textured surfaces significantly can affect the lubrication performance of sliding bearings. Numerous researchers have introduced several mechanisms of load support generation of textured surfaces based on hydrodynamic lubrication theory. Fowell et al. [1] using a mass-conserving numerical analysis stated that any convergence between the bearing surfaces provides a significant mechanism for lift generation. Gherca et al. [2] investigated the influence of the texture geometry using a mass-conserving model. It was concluded that the geometrical features such as size, density, and shape strongly affect the load support. Henry et al. [3] analyzed the influence of surface texturing on the steady-state behavior of bearings experimentally. It was found that the textured bearing reduces friction up to 30% at low loads while for heavy loads, their performance is equivalent or even lower than that of an untextured bearing. Yagi et al. [4] investigated the value of the load support enabled by surface texturing in hydrodynamic lubrication regime. They claimed that the mechanism of load support was strongly affected by boundary condition. In addition, the load support generation could also be enhanced through appropriate partial arrangement of textures [5].

From physical point of view, when the textured surface is applied on the bearing, the inertia as well as the cavitation may exist and affect the lubrication performance. Based on theoretical approach, Safar and Shawki [6] explored the influence of inertia force on the bearing characteristics. They concluded that consideration of inertia effects enhances the hydrodynamic pressure. Although favorable, this effect seems rather insignificant. This finding was also strengthened by Kakoty and Majumdar [7] who concluded that the steady-state characteristic of lubricated is not affected much due to lubricant inertia.



However, Khalil et al. [8] concluded that the inertia force combined with centrifugal force are able to increase the pressure inside the recess and land regions. Syed and Sarangi et al. [9] studied the lubricating performance of textured parallel sliding contacts considering fluid inertia effect. They highlighted that inertia effect is important in altering the lubrication behavior. The interesting result regarding the inertia effect in finite hydrodynamically lubricated textured bearings has been proposed by Woloszynski et al. [10]. Using spectral element solver, it was found that the inertia effect enhances with increasing Reynolds number and decreasing ratio of dimple length to dimple depth.

2. Literature Review

Based on published works, it can be highlighted that most of the solution of the lubrication problems have been solved by ignoring the cavitation phenomena. As is known, when the textured surface is applied on bearing, the cavitation may exist which may decrease or enhance the lubrication performance depending on the texturing parameters. Muchammad et al. [11] studied the effect of cavitation on the hydrodynamic pressure with respect to the inlet suction mechanism on the textured surface including boundary slip. Their main finding was that introducing the slip could retard the presence of cavitation. In recent lubrication, Lin et al. [12] presented the complete analysis regarding with the thermohydrodynamic lubrication model including effects of cavitation and inertia. They showed that inertia and cavitation could reduce the load support and friction. Other interesting result was that the influence of inertia effect on the static characteristics of bearing is larger than the cavitation effect under high speed condition.

Following this main frame, in the present paper a CFD method has been applied to investigate the texturing parameter in particular case of relative texture depth on the hydrodynamic pressure as well as the load support and friction force. The comparison between the analysis considering the cavitation and that without cavitation model is conducted.

3. Research methods and Materials

A. Governing Equations

In the present study, the analysis of lubrication is solved by computational fluid dynamic based on Navier-Stokes equations. These equations are solved over the domain using a finite-volume method with ANSYS FLUENT® software package. The equations are steady and solved in the x- and z-direction only. With these properties the Navier–Stokes and the continuity equations can be expressed, respectively,

$$\rho(\mathbf{u} \cdot \nabla) \mathbf{u} = -\nabla p + \eta \nabla^2 \mathbf{u} \quad (1)$$

$$\nabla \cdot \mathbf{u} = 0 \quad (2)$$

With the application of sliding surfaces in very narrow- gap conditions and the availability of hydrophobic materials, the classical no-slip boundary condition can be break down. When lubricant slips along a solid-liquid interface, the slip length β is generally used to address the relation between slip velocity and surface shear rate, that is,

$$u_s = \beta \left. \frac{\partial u}{\partial z} \right|_{\text{surface}} \quad (3)$$

where u_s indicates the streamwise slip velocity at the slip surface, β denotes the slip length, and $\left. \frac{\partial u}{\partial z} \right|_{\text{surface}}$ is the slip surface is assumed as uniform in space due to the application of a microscopic scale. Numerous studies have shown that the chemical treatment of the surface generates a slip length in the order of 1 μm , whereas longer slip length up to 100 μm can be obtained through a combination of an artificially textured pattern with hydrophobic coating.

Subroutine is developed to enhance capability and customize its feature for a lubrication modeling analysis. This subroutine called as User-Defined-Function (UDF) is a function that allows a user to define the boundary conditions, material properties, and source terms for the flow regime, as well as specify customized model parameters.

In the present work, the flow is considered turbulent. The turbulent model of Realizable k- ϵ is adopted with standard wall functions as near-wall treatment. In the textured bearing, when the flow enters the textured region, pressure might fall below the saturation vapor pressure, and the liquid would rupture and the cavitation occurs. In FLUENT®, there are three available cavitation models: Schmeer and Sauer model, Zwart-Gelber-Belamri model and Sighal et al. Model [13]. In this study, the Zwart-Gelber-Belamri is used due to their less sensitive to mesh density, robust and converge quickly [13]. In cavitation, the liquid- vapor mass transfer is governed by the vapor transport equation [13]:

$$\frac{\partial}{\partial t}(\alpha_v \rho_v) + \nabla \cdot (\alpha_v \rho_v \mathbf{v}) = R_g - R_c \quad (4)$$

where α_v is vapour volume fraction and ρ_v is vapor density. R_g and R_c account for the mass transfer between the liquid and vapour phases in cavitation. For Zwart-Gelber-Belamri model, the final form of the cavitation is as follows:

$$\text{If } p \leq p_v, R_g = F_{\text{evap}} \frac{3\alpha_{\text{nuc}}(1-\alpha_v)\rho_v}{R_B} \sqrt{\frac{2P_v - P}{3\rho_l}} \quad (5)$$

$$\text{If } p \geq p_v, R_c = F_{\text{cond}} \frac{3\alpha_v \rho_v}{R_B} \sqrt{\frac{2P - P_v}{3\rho_l}} \quad (6)$$

where F_{evap} = evaporation coefficient = 50, F_{cond} = condensation coefficient = 0.01, R_B = bubble radius = 10^{-6} m, α_{nuc} = nucleation site volume fraction = 5×10^{-4} , ρ_l = liquid density and p_v = vapour pressure

B. CFD Model and Boundary Condition

The schematic representation of textured bearing is shown in Fig. 1. The textured surface is composed of a single macro texture cell with wall slip. For the analysis, the wall slip is engineered to occur at the leading edge of the contact. For all the following simulations, the standard one- dimensional textured bearing geometry is investigated, with values for the parameter as presented in Table 1.

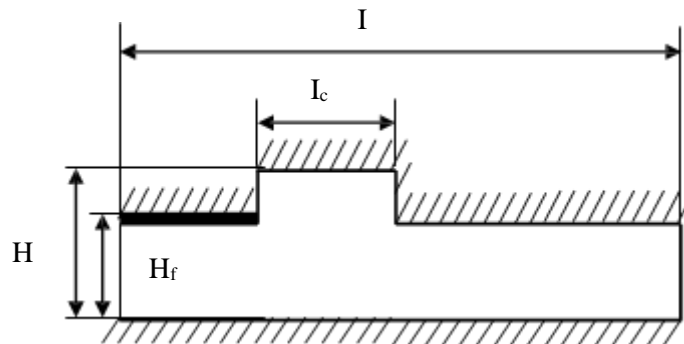


Figure 1. Geometry model of textured lubricated contact with slip

Table 1. Characteristic of textured bearing parameter

Parameter	Symbol	Value	Unit
Length of bearing	l	2.00	mm
Length of slip region	l_s	0.50	mm
Length of texture cell	l_c	0.50	mm
Density of oil	ρ	1000	kg/m ³
Density of vapor	ρ	0.001	kg/m ³
Viscosity of oil	μ_o	0.013468	kg/ms
Viscosity of vapor	μ	1.256×10^{-5}	kg/ms
Atmospheric pressure	p_{atm}	101.33	kPa
Cavitation pressure	p_{cav}	3.54	kPa
Slip coefficient	α	0.02	m ² /s/kg

In the present study, the effect of texturing on the hydrodynamic pressure of the lubricated contact is investigated. As noted, according to Dobrica and Fillon [14], a texture cell is in detail defined by three non-dimensional parameters: relative texture depth, texture aspect ratio and the texture density. In this work, the relative texture depth K (defined as ratio between the texture depth h_d and the land film thickness h_f , as seen in Fig. 2) is of particular interest. For all following computations studied here, it is assumed that both the relative texture depth and the texture aspect ratio is constant and equal to 0.5, while the relative texture depth K is varied to 10, 4, and 2. In this discussion, the variation of K is conducted by modifying the land film thickness h_f while keeping a constant h_d .

The CFD models are meshed using hexahedron grids. In the present work, a mesh refinement study is performed to produce more accurate solutions. Fig. 2 reflects the schematic representation of mesh of domain. In certain local region, the mesh is refined with the computational points added only in parts of the domain where higher resolution is necessary. In the present work, the entire computational domain is fully flooded. As a consequence, lubricant pressure at the inlet and outlet sections of the bearing is set to zero atmospheric gauge pressure as indicated in Table 1. The lower surface is set to be moving, and the upper surface is set to be static. The hydrodynamic pressure profile and cavitation position are calculated in the MIXTURE model, and as implied multiple-phase flow is employed to investigate the gas-liquid mixture flow under the cavitation situation. At the leading edge of the contact, the wall slip is applied.

The second order upwind discretization scheme is used for the momentum equations and the QUICK discretization scheme is used for the volume fraction equation. In the present study, a convergence tolerance of 10^{-6} is used for all residual terms to obtain the greater accuracy. All numerical calculations are performed using FLUENT package. For solving the analysis, finite volume forms of the continuity and momentum equations are applied. A steady-state incompressible solver is used. The SIMPLEC algorithm is adopted to treat the pressure-velocity coupling.

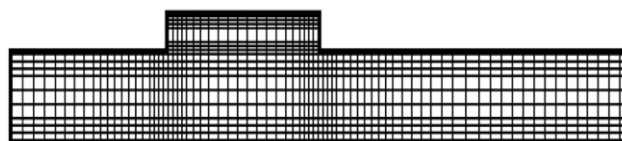


Figure 2. Mesh of geometry model

4. Results and discussion

Fig. 3 shows the hydrodynamic pressure along the surface area varying the relative texture depth K for two different situations (i.e. with considering cavitation model and without considering cavitation model) for the case of Reynolds number $Re = 100$. It can be seen that the cavitation model has a huge impact on the hydrodynamic pressure especially for the K of 4. There is a big deviation of the prediction of hydrodynamic pressure between the solution considering cavitation model and that without considering model. For other values of K studied here, that is $K = 10$ and $K = 2$, it seems that consideration of cavitation model in the analysis does not affect the hydrodynamic pressure very much. For the low K (in this case $K = 2$), the predicted pressure distributions between two methods (i.e. cavitation versus no-cavitation) show the same profile. Based on the physical point of view, it can be observed that when the ratio of texture depth over the land film thickness is not so high or so low, the cavitation phenomena may exist in the textured lubricated contact, and therefore the cavitation model should take into account in the analysis.

Based on Fig. 3, it can be seen that there is an optimum value of relative texture depth K related to cavitation effect. If the relative texture depth K is higher or lower than this optimum value, the hydrodynamic response improves abruptly. One can remark that when the textured contact with optimal relative texture depth, the presence of the cavitation leads to improved the hydrodynamic pressure significantly, and thus the enhanced load support. The most possible explanation is that there may be a mechanism of inlet suction of the lubricant due to cavitation as discussed by Fowell et al. [1], and as a consequence the load support is increased.

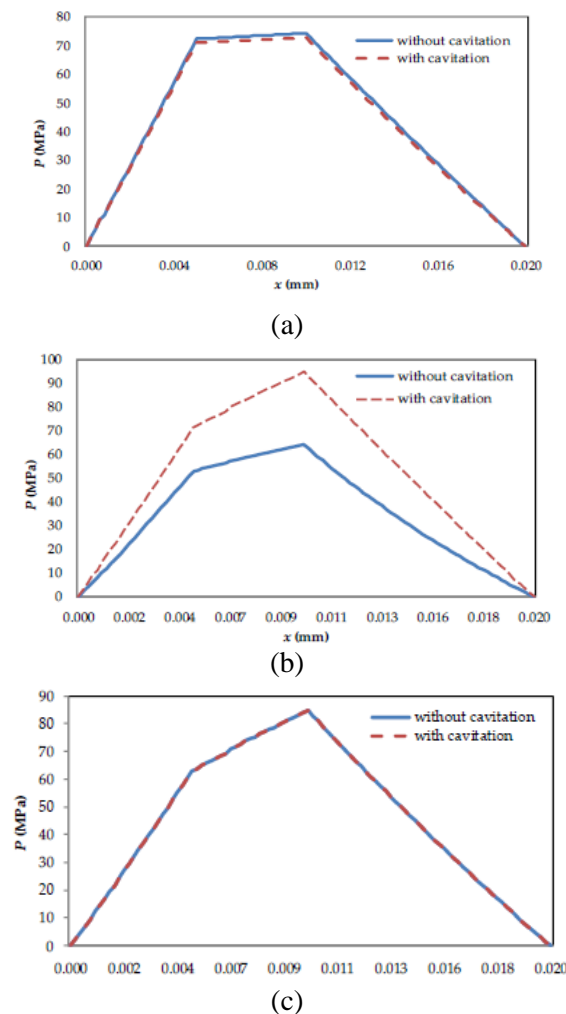


Figure 3. Comparison of hydrodynamic pressure distributions between cavitation and no-cavitation conditions in the case of $Re = 100$ for: (a) relative texture depth K of 10; (b) relative texture depth K of 4; (c) relative texture depth K of 2.

In more detail, the correlation between the relative texture depth K and the hydrodynamic performance is shown in Fig. 4. Two observations can be made based on Fig. 4 (a) and (b). Firstly, in the case of analysis considering cavitation model, increasing the relative texture depth does not necessarily enhance or reduce the hydrodynamic pressure. As discussed in previous section, there is an optimal value of K with respect to the hydrodynamic pressure. Secondly, it can be observed that in texturing area, the pressure profile for the case of $K = 4$ has higher value than others. The opposite result is found when the analysis is carried out by not taking into account the cavitation model. For the case of $K = 4$, the much lower hydrodynamic pressure is highlighted.

On the other words, when the cavitation occurs in such contact, the analysis without cavitation model can not capture the lubricant behavior. What so-called under-estimated prediction of pressure may be found when one neglects the cavitation model in analyzing the textured contact. Fig. 5 shows the hydrodynamic pressure varying the relative texture depths for the case of Reynolds number of 200.

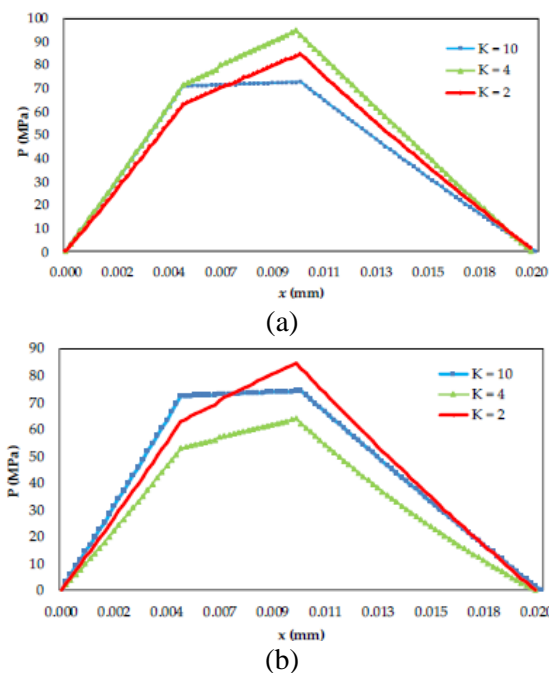
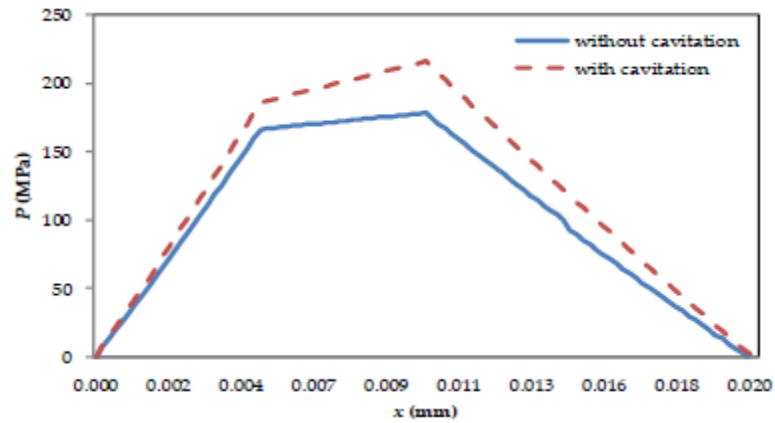


Figure 4. Hydrodynamic pressure distributions for different values of relative texture depth in the case of $Re = 100$: (a) considering cavitation model; (b) without considering cavitation model

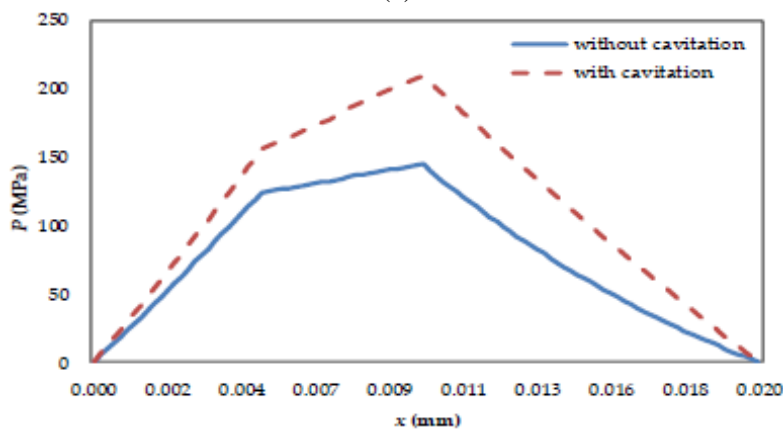
It can be observed that the smaller the relative texture depth, the larger the deviation of the prediction of the hydrodynamic pressure between that considering cavitation model and that without considering cavitation model. It is also highlighted that for all value of relative texture depth considered here the solution with cavitation model gives higher pressure distribution compared to that without cavitation model. From the physical point of view, increasing the relative texture depth K for the Reynolds number of 200 can trigger the occurrence of cavitation. It seems that there is a strong correlation between the inertia and the cavitation. For lower Re ($Re = 100$, in this case), the cavitation does not occur at the bearing with $K = 10$ and $K = 2$. For higher Reynolds number (i.e. $Re = 200$) which leads to more inertia effect, the cavitation is found for all value of K here. However, the hydrodynamic pressure profiles generated is in the positive perspective, which means that the cavitation enhance the load support.

Another interesting feature from Fig. 5 is that when the cavitation exists in textured contacts studied here, the inertia may have a dominant role in altering the lubricant behavior. For lubricated contact with low K ($K = 2$ in this case), the hydrodynamic pressure distribution is higher over the surface area both for the case of “with cavitation mode” and the case of “without cavitation model” as respectively observed in more detail based on Fig. 6 (a) and (b). The most possible explanation is that from the

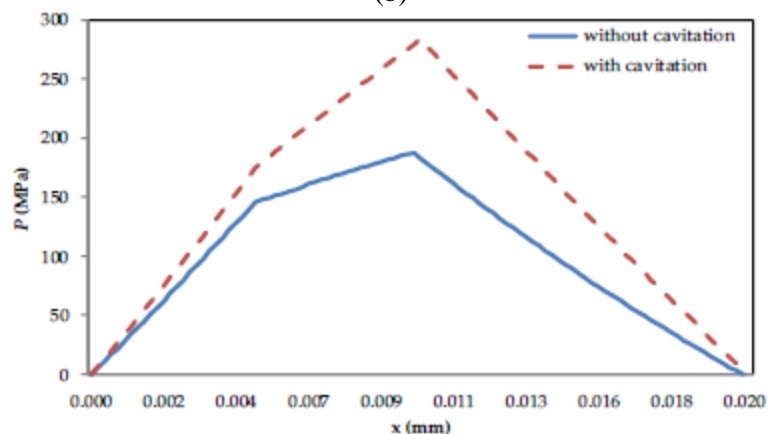
geometrical point of view, the vortex in textured bearing with K of 2 has a higher possibility to occur due to low ratio of texture depth over land film thickness.



(a)



(b)



(c)

Figure 5. Comparison of hydrodynamic pressure distributions between cavitation and no-cavitation conditions in the case of $Re = 200$ for: (a) relative texture depth K of 10; (b) relative texture depth K of 4; (c) relative texture depth K of 2.

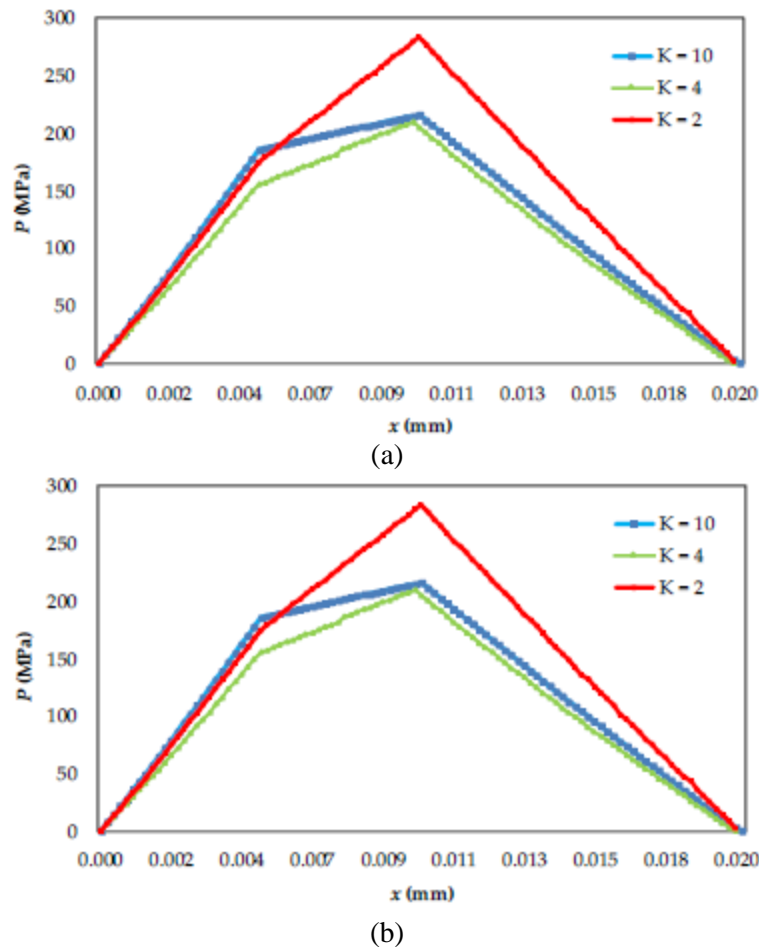


Figure 6. Hydrodynamic pressure distributions for different values of relative texture depth in the case of $Re = 200$: (a) considering cavitation model; (b) without considering cavitation model.

5. Conclusion

In the present study, the lubrication analysis of the single textured-slip bearing was solved by the Navier-Stokes Equation using CFD software. The Navier-slip model was used to model the slip. The comparison between the analysis considering the cavitation model and that without considering the cavitation model was of particular interest. Based on the explanation discussed earlier, the conclusion can be drawn as follows:

1. The cavitation has a significant effect on altering the hydrodynamic performance of bearing and thus the cavitation model should be considered in analysis to obtain the correct prediction of the flow behavior in bearing.
2. The main finding is that for slip-textured pattern there is an optimum value of relative texture depth related to cavitation effect. If the relative texture depth is higher or lower than this optimum value, the hydrodynamic response improves abruptly due to the presence of cavitation.

References

- [1]. M.T. Fowell, S. Medina, A.V. Olver, H.A. Spikes, I.G. Pegg, "Parametric study of texturing in convergent bearings," *Tribol Int.*, vol. 2012, 52, pp. 7–16.

- [2]. A.R. Gherca, P. Maspeyrot, M. Hajjam, A. Fatu, "Influence of texture geometry on the hydrodynamic performances of parallel bearings," *Tribology Trans.*, vol. 56, 2013, no. 3, pp. 321-332.
- [3]. Y. Henry, J. Bouyer, M. Fillon, "An experimental analysis of the hydrodynamic contribution of textured thrust bearings during steady-state operation: A comparison with the untextured parallel surface configuration," *Proc Inst MechEng Part J: J EngTribol*, 2015, 229 (4), pp. 362–375.
- [4]. K. Yagi, H. Sato, J. Sugimura, "On the magnitude of load-carrying capacity of textured surfaces in hydrodynamic lubrication." *Tribol Online* 2015, 10(3), pp. 232-245.
- [5]. Zhang, H.; Dong, G.; Hua, M.; Guo, F.; Chin, K.S. Parametric design of surface textures on journal bearing *Ind LubrTribol* 2015, 67 (4), pp.359-369.
- [6]. Z.S. Safar and G.S.A. Shawki, "Do convective inertia forces affect turbulent bearing characteristics?," *Tribol Int.* 1978, 11 (4), pp. 248-249.
- [7]. S.K. Kakoty and B.C. Majumdar, "Effect of fluid inertia on stability of flexibly supported oil journal bearings: linear perturbation analysis," *Tribol Int.* 1999, 32, pp. 217–228.
- [8]. M.F. Khalil, S.Z. Kassab, A.S. Ismail, "Influence of inertia forces on the performance of turbulent externally pressurized bearings," *Tribol Int.*, 1992, 25 (1), pp. 17-25.
- [9]. I. Syed and M. Sarangi, "Hydrodynamic lubrication with deterministic microtextures considering fluid inertia effect," *Tribol Int.*, 2014, 169, pp. 30–38.
- [10]. Woloszynski, T.;Podsiadlo, P.;Stachowiak, G.W. Evaluation of inertia effect in finite hydrodynamic bearings with surface texturing using spectral element solver. *Tribol Int* 2015, 91, pp. 170–176.
- [11]. M. Muchammad, M. Tauviriqirrahman, J. Jamari, D.J. Schipper, "An analytical approach on the tribological behaviour of pocketed slider bearings with boundary slip including cavitation," *Lubr Sci* 2017, 29, pp. 133–152.
- [12]. X. Lin, S. Jiang, C. Zhang, X. Liu, "Thermohydrodynamic analysis of high speed water-lubricated spiral groove thrust bearing considering effects of cavitation, inertia and turbulence," *Tribol Int.* 2018, 119, pp. 645–658.
- [13]. ANSYS, ANSYS Fluent, version 14.0: user manual. ANSYS, Inc., Canonsburg, USA., 2011.
- [14]. M.B. Dobrica and M. Fillon, "About the validity of Reynolds equation and inertia effects in textured sliders of infinite width," *Proc Inst Mech Eng Part J: J EngTribol* 2009, 223, pp. 69-78.
- [15]. F. Sahlin, S.B. Glavatskih, T. Almqvist, "Larsson, R. Two-dimensional CFD-analysis of micro-patterned surfaces in hydrodynamic lubrication," *ASME J Tribol* 2005, 12, pp. 96-102.